

Fully relativistic two-component-spinor approach in the ultrasoft-pseudopotential plane-wave method

著者	Oda Tatsuki, Hosokawa Akihiko
journal or publication title	Physical Review B - Condensed Matter and Materials Physics
volume	72
number	22
page range	224428
year	2005-12-01
URL	http://hdl.handle.net/2297/3463

Fully relativistic two-component-spinor approach in the ultrasoft-pseudopotential plane-wave method

Tatsuki Oda and Akihiko Hosokawa

Graduate School of Natural Science and Technology, Kanazawa University, Kanazawa 920-1192, Japan

(Received 9 August 2005; published 21 December 2005)

We have introduced effects of spin-orbit interaction nonperturbatively to the ultrasoft-pseudopotential scheme accompanied by two component spinor wave functions. Application to the electronic structure calculations of some heavy elements successfully reproduced results of the all electron approaches. The magnetic anisotropy energy and the orbital magnetic moment for alloys, which have shown a good agreement with the previous results, demonstrated broad capabilities of the approach.

DOI: [10.1103/PhysRevB.72.224428](https://doi.org/10.1103/PhysRevB.72.224428)

PACS number(s): 75.30.Gw, 71.15.Dx, 71.15.Rf

I. INTRODUCTION

Spin-orbit interaction (SOI) is a relativistic effect on electrons and is included automatically by solving the Dirac equation.¹ In electronic structure calculations, this effect has been introduced by a direct treatment or a perturbative approach for the Dirac equation. In density functional approaches to the system which requires SOI, all electron approaches have been popular, while the pseudopotential approach has a potential to study structural and dynamical properties of systems for heavy elements.

Recently, the self-consistent treatment of bispinor wave functions was used for the study on the dilute magnetic semiconductors.^{2,3} For the heavy elements, Corso *et al.* developed a relativistic ultrasoft pseudopotential (USPP) and reported the application to Au and Pt bulk systems.⁴ For those materials which include heavy elements, details of the electronic structure depend on the SOI, reflecting on, for example, structural properties of material. As another important issue, SOI is an origin of magnetic anisotropy for magnetic materials.

In this work, we implemented the electronic structure calculations by using the fully relativistic pseudopotential⁵ for the bispinor Kohn-Sham equation.⁶ For the application to nonmagnetic materials, we presented spin-orbit effects explicitly on the electronic band structure and, for magnetic materials, we challenged to estimating the magnetic anisotropy energy (MAE) for CoPt and FePt. To treat such materials that contain transition metal elements, the USPP has been an important device for the plane-wave method.⁷ The present scheme, which has been coded in line of the Car-Parrinello method,⁸ is essentially the same as previously published.⁴ As a result of implementation, we believe that the scheme has a potential to study effects of SOI with a wide range of freedom by combining the molecular dynamics.⁹

II. FORMALISM

The theoretical formulation is based on the bispinor wave function Ψ_i , which has two components, ψ_{i1} and ψ_{i2} , where the index i specifies an orbital among the set of Kohn-Sham orbitals $\{\Psi_j\}$.¹⁰⁻¹³ Each component is expanded with plane-wave basis set. The electron density $n(\mathbf{r})$, and the spin density $\mathbf{m}(\mathbf{r})$ are found by expanding the density matrix, ρ , as

follows; $\rho(\mathbf{r}) = n(\mathbf{r})\sigma_0/2 + \sum_k m_k(\mathbf{r})\sigma_k/2$, where σ_0 and σ_k ($k=x, y, z$) are the unit and the Pauli spin matrices, respectively. The elements of the density matrix are given by

$$\rho_{\alpha\beta}(\mathbf{r}) = \sum_i f_i \left\{ \psi_{i\alpha}(\mathbf{r})\psi_{i\beta}^*(\mathbf{r}) + \sum_{pq\ell} Q_{pq,\alpha\beta}^{\ell} \langle \beta_p^{\ell} | \Psi_i \rangle \langle \Psi_i | \beta_q^{\ell} \rangle \right\}, \quad (1)$$

where f_i is the occupation number of the i th Kohn-Sham orbital and the second term in parentheses corresponds to a localized part of the electron density, which is peculiar to the USPP scheme.^{14,15}

For each atom, this term augments the electron density by using localized charge density functions $Q_{pq,\alpha\beta}^{\ell}(\mathbf{r})$ and projector functions $\beta_p^{\ell}(\mathbf{r})$, centered at the nuclear position. In the relativistic formulation, $\beta_p^{\ell}(\mathbf{r})$ has the spinor form,

$$\beta_p^{\ell}(\mathbf{r}) = \beta_{j\kappa\tau}^{\ell}(r) \mathcal{Y}_{j,\mu}^{\text{sgn}(\kappa)}(\hat{\mathbf{r}}), \quad (2)$$

where the indices of j, μ , and κ are the atomic relativistic quantum numbers and the index of p specifies the combined one, $p = \{j, \mu, \kappa, \tau\}$. The last index of τ specifies the number of augmentation for reproducing scattering properties of the realistic atom in an all-electron calculation.¹⁴ The spin-angular harmonic function $\mathcal{Y}_{j,\mu}^{\text{sgn}(\kappa)}$ can be defined, depending on the quantum number, for $j = \ell + (1/2)$, $\mu = m + (1/2)$ ($\kappa = -\ell - 1 < 0$), as follows:

$$\mathcal{Y}_{j,\mu}^{-}(\hat{\mathbf{r}}) = \sqrt{\frac{\ell+m+1}{2\ell+1}} Y_{\ell,m}(\hat{\mathbf{r}}) \begin{pmatrix} 1 \\ 0 \end{pmatrix} + \sqrt{\frac{\ell-m}{2\ell+1}} Y_{\ell,m+1}(\hat{\mathbf{r}}) \begin{pmatrix} 0 \\ 1 \end{pmatrix}, \quad (3)$$

and for $j = \ell - (1/2)$, $\mu = m - (1/2)$ ($\kappa = \ell > 0$),

$$\mathcal{Y}_{j,\mu}^{+}(\hat{\mathbf{r}}) = \sqrt{\frac{\ell-m+1}{2\ell+1}} Y_{\ell,m-1}(\hat{\mathbf{r}}) \begin{pmatrix} 1 \\ 0 \end{pmatrix} - \sqrt{\frac{\ell+m}{2\ell+1}} Y_{\ell,m}(\hat{\mathbf{r}}) \begin{pmatrix} 0 \\ 1 \end{pmatrix}, \quad (4)$$

where $Y_{\ell,m}$ is the spherical harmonic function.

The augmented charge density of $Q_{pq,\alpha\beta}^{\ell}(\mathbf{r})$ has a 2×2 matrix form in the spinor indices. As in the original approach,⁷ the function has the pseudized form,

$$Q_{pq,\alpha\beta}^I(\mathbf{r}) = \sum_{LM} C_{pq}^{LM} Q_{pq,\alpha\beta}^{I,LM}(r) Y_{LM}(\hat{\mathbf{r}}), \quad (5)$$

where C_{pq}^{LM} is a coefficient induced by the Clebsch-Gordan coefficients.

In practice, this scheme is easily developed from the non-collinear scheme which has been implemented previously.^{6,9} The formalisms of the Kohn-Sham energy (E_{tot}) and the Kohn-Sham equation are written down by replacing the atomiclike orbitals to the relativistic version (β_p^I), paying attention to the spinor matrix form of $Q_{pq,\alpha\beta}^I(\mathbf{r})$. In E_{tot} , the nonlocal part of pseudopotential V_{NL} is given by

$$V_{\text{NL}} = \sum_{pql} |\beta_q^I\rangle D_{pq}^{(0)I} \langle \beta_p^I|. \quad (6)$$

The quantities $\beta_p^I(\mathbf{r})$, $D_{pq}^{(0)I}$, $Q_{pq,\alpha\beta}^I(\mathbf{r})$, and $V_{\text{loc}}^{\text{ion}}(\mathbf{r})$ characterize the USPP and are obtained from calculations for an isolated atom.^{5,14} The last quantity $V_{\text{loc}}^{\text{ion}}(\mathbf{r})$ is the local part of pseudopotential. Compared with the previous scheme,⁹ the number of local orbitals (β_p^I) is increased twice. In our implementation, the augmented density $Q_{pq,\alpha\beta}^I(\mathbf{r})$ has been pseudized, allowing the interested system to become larger in applications.

The target systems in the present work are metallic, treating the occupation number of f_i as noninteger values in the vicinity of the Fermi level. According to this, for a self-consistent treatment, we used the functional form,^{16,17} $F_{\text{tot}} = E_{\text{tot}} - S_{\text{el}}/\beta$, where S_{el}/β is an entropic energy of an electron and $1/\beta$ specifies a scale of energy width for smearing at the Fermi level. The self-consistent solution is obtained by minimizing the energy functional of F_{tot} .

III. PSEUDOPOTENTIAL PREPARATION

The present scheme requires a relativistic version of USPPs. The relativistic effect including spin-orbit interaction can be taken into account by solving the Dirac equation for the part of an all-electron calculation and introducing the j -dependent atomiclike radial function instead of the ℓ -dependent function in the conventional scheme.¹⁴ Following the previous works,^{18,19} in which they neglected the minor component of radial wave function at the radius far from the nuclei, we only considered the major component for pseudo-wave function. This approximation could be assumed for a wide variety of elements. Additionally, it allows us to use almost all parts of the scalar relativistic (conventional) USPP generation code¹⁴ without complex cumbersome modifications.

For an open shell, the electron occupation at each atomic level is distributed in the ratio of multiples in the j -dependent level. For lead, the atomic energy levels obtained agree with the results in the previous work.¹⁹ The details of generation will be published elsewhere.⁵

The relativistic version of USPP for Fe is generated with the similar parameters used in the previous work.⁶ For Co, we generated the pseudopotential in a similar way as Fe, but used the ionic reference state consisting of $(3d)^7(4s)^1(4p)^{0.5}$

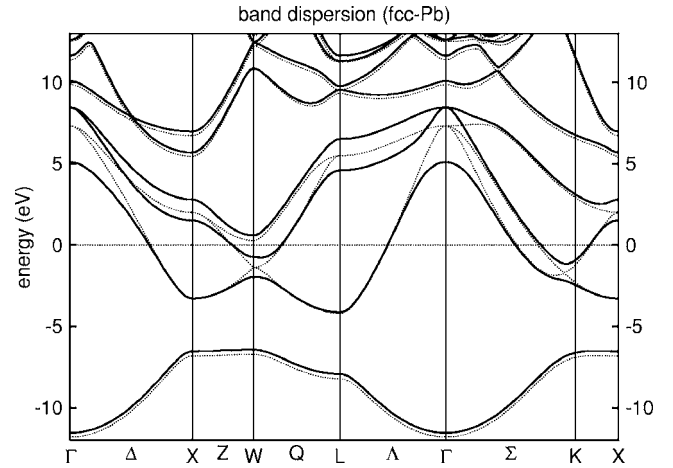


FIG. 1. Band dispersions of lead. The thick and thin curves represent dispersions of fully relativistic and scalar relativistic cases, respectively. The dispersions for the $5d$ state are not shown.

valence electrons with $3s$ - and $3p$ -semicore electrons. The exchange-correlation form of Cepaly-Alder-Perdew-Zunger is used in this work.²⁰

IV. APPLICATION

A. Band calculations for lead, gold, and platinum

The typical heavy metal is an application for demonstrating the developed scheme. We applied to lead and the two noble metals of gold and platinum, all that have a fcc crystal structure. We took in the plane-wave basis the energy cutoffs of 40 and 300 Ry for wave functions and charge densities, respectively. The sampling \mathbf{k} points of Monkhost and Pack with the $10 \times 10 \times 10$ mesh was used for constructing the self-consistent densities $\rho(\mathbf{r})$.²¹ The Fermi-Dirac distribution function with $1/\beta$ of 27 meV was taken into account in the smearing at the Fermi level.

The band dispersions are presented at the experimental lattice constant for lead in Fig. 1. The spin-orbit splittings are found remarkably around the Γ , W , and K points, while the SOI does not affect eigenvalues so largely at the Fermi level for this material. The eigenvalues of the fully relativistic version at typical \mathbf{k} points are compared with the previous calculation and experimental data in Table I. Our results are in good agreement with the all-electron approaches.²² For gold and platinum, it was also found that the band dispersions (not shown) were very similar to the results of the previous theoretical works.^{4,25}

Table II presents the equilibrium lattice constant and the bulk modulus for lead, gold, and platinum, compared with the experimental data. Concerned with the lattice constant, the agreement with experiment is within 0.6%. For the bulk modulus, our result shows the larger values than the values of experiment, which is similar to the result of other theoretical calculations. In Table II, the effect of SOI (difference between SR and FR) is relatively large (6%) for the bulk modulus of lead. On the whole, however, the SOI does not change the physical quantities so significantly.

TABLE I. Eigenvalues (in eV) of a fully relativistic version at the typical \mathbf{k} points for lead, compared with the all-electron approach. USPP specifies results of the present work and the values in parentheses were measured by the angle-resolved photoelectron spectroscopy.

\mathbf{k}	USPP	RAPW ^a (exp. ^b)	\mathbf{k}	USPP	RAPW ^a (exp. ^b)
Γ	-11.55	-11.4 (-11.4)	W	-6.43	-7.2
	5.10			-1.97	
	8.48			-0.73	
L	-7.92	-8.2	X	-6.52	-6.7 (-6.8)
	-4.13	-4.5		-3.28	-3.6 (-3.4)
K	-6.61	-6.7 (-6.9)			
	-2.44	-2.8 (-2.7)			
	-0.93	-1.2 (-1.0)			

^aReferences 22 and 23.

^bReferences 24.

B. Magnetic anisotropy energy for FePt and CoPt

To demonstrate the fully relativistic approach, MAE is one of good physical quantities. The SOI mainly contributes this quantity. CoPt and FePt are the typical materials to study in the previous theoretical approach.²⁷⁻³⁰

The structure of present calculations has an ordered atomic arrangement of a fcc alloy, in which the same element distributes in the same (001) layer, alternatively. The unit cell of the calculation has a magnetic atom (Co or Fe) at the origin and a platinum atom at the center of the tetragonal cell. The experimental lattice constants are used in the calculation: $a=5.08$, $c=7.01$ a.u. for CoPt, and $a=5.16$, $c=7.15$ a.u. for FePt.²⁹ Both parameters correspond to slightly compressed cells along the c axis with respect to an ideal fcc lattice.

We estimated the total energy difference as the MAE; $F_{\text{tot}}[110]-F_{\text{tot}}[001]$, where the direction in the square brackets specifies the magnetization direction in the tetragonal lattice. To estimate the MAE in the bulk materials, it is necessary to include a large number of \mathbf{k} sampling points, as in the previous study.²⁹ We used the $22 \times 22 \times 22$ mesh for \mathbf{k} space, resulting in 10 648 points. We also used the same conditions

TABLE II. The equilibrium lattice constant (a) and the bulk modulus (B_0) for lead, gold, and platinum, compared with the data of an all-electron approach (AE) and the experimental data (exp.). SR and FR specify the cases of scalar relativistic and fully relativistic pseudopotentials, respectively.

	a (a.u.)					B_0 (GPa)				
	SR	FR	FR ^a	AE ^b	exp. ^c	SR	FR	FR ^a	AE ^b	exp. ^c
Pb	9.27	9.30			9.35	48.6	45.6			43.0
Au	7.68	7.66	7.64	7.637	7.71	194	198	198.1	195	173.2
Pt	7.42	7.43	7.40	7.370	7.41	300	296	292.0	297	278.3

^aReferences 4.

^bReferences 25.

^cReferences 26.

TABLE III. Magnetic anisotropy energy (MAE) and the total spin magnetic moment for CoPt and FePt. The latter is presented for values of the [001] magnetization.

	MAE (meV/f.u.)		m_s (μ_B)			
	USPP	AE	USPP	AE		
CoPt	0.52	1.5 ^a	1.052 ^b	2.28	2.29 ^a	2.146 ^b
FePt	2.61	2.8 ^a	2.734 ^b	3.33	3.26 ^a	3.205 ^b

^aReferences 28.

^bReferences 29.

for the energy cutoffs and the Fermi level smearing as in the previous section of nonmagnetic bulks.

The MAE and the total spin magnetic moment are presented in Table III, compared with the data of all-electron approaches. In both materials, the magnetic easy axis is correctly predicted, and the data estimated for [100] magnetization (not reported here) are very similar to that of [110]. The latter implies a small anisotropy within (001) planes. Our MAE of FePt is in good agreement with the value of all-electron approaches. For CoPt, the MAE obtained is smaller than the values of the all electron. The previous values estimated from theoretical and experimental approaches are still dispersive in a relatively wide range, and the effect of orbital polarization which has been ignored here should improve the MAE in CoPt.²⁹

In Table IV, we compare our result with the previous data on atomic magnetic moments. The formalism for the orbital moment, which is described in the Appendix, is based on the work in Ref. 31. Overall agreement is very satisfactory, compared with all-electron approaches. The result is presented for two magnetization directions of [001] and [110]. For CoPt, the orbital moment in Co is largely decreased from [001] magnetization to [110], while the moment in Pt is increased. Interestingly, the above relation in orbital moment between [001] and [110] is observed also in the all-electron calculation. This kind of agreement, although the change in orbital moment is small, is also true for FePt.

TABLE IV. Atomic spin and orbital magnetic moments (in μ_B) for CoPt and FePt. The radius of 2.5 a.u. was used for all atomic spheres. The magnetization direction is specified in square brackets.

	Spin		Orbital	
	USPP	AE	USPP	AE
CoPt Co	1.926	1.91 ^a 1.803 ^b	0.102	0.11 ^a 0.089 ^b
[001] Pt	0.377	0.38 ^a 0.394 ^b	0.061	0.07 ^a 0.056 ^b
CoPt Co	1.929	1.809 ^b	0.069	0.057 ^b
[110] Pt	0.377	0.398 ^b	0.078	0.073 ^b
FePt Fe	3.016	2.93 ^a 2.891 ^b	0.067	0.08 ^a 0.067 ^b
[001] Pt	0.338	0.33 ^a 0.353 ^b	0.046	0.05 ^a 0.042 ^b
FePt Fe	3.020	2.893 ^b	0.062	0.061 ^b
[110] Pt	0.340	0.355 ^b	0.059	0.055 ^b

^aReferences 28.

^bReferences 29.

V. CONCLUSION

The SOI was introduced in the USPP scheme accompanied by two component spinor wave functions. The application to the simple metal consisting of the heavy elements successfully reproduced the results of all-electron approaches. Our fully relativistic scheme was tested in estimating the MAE and orbital magnetic moment for alloys, CoPt and FePt. The present work implies a considerable potential in the pseudopotential plane-wave method to study the magnetic anisotropy as well as the structural and dynamical properties in relativistic systems.

ACKNOWLEDGMENTS

The computation in this work was partially carried out using the facilities of the Super computer Center, Institute for Solid State Physics, University of Tokyo. This work has been partially supported by the Japan Society for the Promotion of Science (JSPS) under Project No. 16310081. One of the authors (T.O.) would like to thank the JSPS for financial support (Project No. 17540292).

APPENDIX A: ORBITAL MAGNETIC MOMENT

We present the formalism of an orbital magnetic moment in the USPP method. The average of the orbital angular momentum operator at l th atomic sphere can be written as follows:

$$\langle \ell_k \rangle_l = \langle \ell_k \rangle_{l,PW} + \langle \ell_k \rangle_{l,VB} \quad (k = x, y, z), \quad (A1)$$

$$\langle \ell_k \rangle_{l,PW} = \sum_i f_i \langle \Psi_i | \ell_k | \Psi_i \rangle_l, \quad (A2)$$

$$\langle \ell_k \rangle_{l,VB} = \sum_{ipq} f_i \langle \Psi_i | \beta_q^l \ell_{k,pq}^l \beta_p^l | \Psi_i \rangle. \quad (A3)$$

The contribution is divided into two parts, namely, the plane-wave part $\langle \ell_k \rangle_{l,PW}$ and the augmented (Vanderbilt's) part $\langle \ell_k \rangle_{l,VB}$. The expectation value, $\langle \Psi_i | \ell_k | \Psi_i \rangle_l$, can be calculated by using the expansion of the wave function at the l th atomic site;

$$\psi_{i\alpha}(\mathbf{r}) = \sum_{\ell m} Y_{\ell m}(\hat{\mathbf{r}}_l) R_{\ell m, i\alpha}(r_l). \quad (A4)$$

For applications in the text, we included ℓ up to two. The matrix element $\ell_{k,pq}^l$ on local orbitals is presented by

$$\ell_{k,pq}^l = \int_0^{r_c} \phi_{j_1 \kappa_1 \tau_1}(r_l) \phi_{j_2 \kappa_2 \tau_2}(r_l) r_l^2 dr_l \langle \mathcal{Y}_{j_2 \mu_2}^{\text{sgn}(\kappa_2)} | \ell_k | \mathcal{Y}_{j_1 \mu_1}^{\text{sgn}(\kappa_1)} \rangle, \quad (A5)$$

where the indices of p and q are read as the composites of $\{j_1, \mu_1, \kappa_1, \tau_1\}$ and $\{j_2, \mu_2, \kappa_2, \tau_2\}$, respectively. The radial integral in Eq. (A5) can be found in the generation process on the Fourier component for $Q_{pq, \alpha\beta}^l(\mathbf{r})$.

¹P. A. M. Dirac, *The Principles of Quantum Mechanics*, 4th ed. (Misuzu Shobo, Tokyo, 1963).

²G. Theurich and N. A. Hill, Phys. Rev. B **64**, 073106 (2001).

³G. Theurich and N. A. Hill, Phys. Rev. B **66**, 115208 (2002).

⁴A. D. Corso and A. M. Conte, Phys. Rev. B **71**, 115106 (2005).

⁵A. Hosokawa and T. Oda (unpublished).

⁶T. Oda, A. Pasquarello, and R. Car, Phys. Rev. Lett. **80**, 3622 (1998).

⁷K. Laasonen, A. Pasquarello, R. Car, C. Lee, and D. Vanderbilt, Phys. Rev. B **47**, 10142 (1993).

⁸R. Car and M. Parrinello, Phys. Rev. Lett. **55**, 2471 (1985).

⁹T. Oda and A. Pasquarello, Phys. Rev. B **70**, 134402 (2004).

¹⁰P. Hohenberg and W. Kohn, Phys. Rev. **136**, B864 (1964); W. Kohn and L. J. Sham, *ibid.* **140**, A1133 (1965).

¹¹U. von Barth and L. Hedin, J. Phys. C **5**, 1629 (1972).

¹²J. Kübler, K. H. Höck, J. Sticht, and A. R. Williams, J. Phys. F: Met. Phys. **18**, 469 (1988).

¹³J. Kübler, *Theory of Itinerant Electron Magnetism* (Oxford University Press Inc., New York, 2000), p. 56.

¹⁴D. Vanderbilt, Phys. Rev. B **41**, 7892 (1990); the recent development is opened at <http://www.physics.rutgers.edu/~dhv/uspp/index.html>.

¹⁵A. Pasquarello, K. Laasonen, R. Car, C. Lee, and D. Vanderbilt,

Phys. Rev. Lett. **69**, 1982 (1992).

¹⁶M. Weinert and J. W. Davenport, Phys. Rev. B **45**, 13709 (1992).

¹⁷T. Oda, J. Phys. Soc. Jpn. **71**, 519 (2002).

¹⁸L. Kleinman, Phys. Rev. B **21**, 2630 (1980).

¹⁹G. B. Bachelet and M. Schlüter, Phys. Rev. B **25**, 2103 (1982).

²⁰J. P. Perdew and A. Zunger, Phys. Rev. B **23**, 5048 (1981).

²¹H. J. Monkhost and J. D. Pack, Phys. Rev. B **13**, 5188 (1976).

²²T. L. Loucks, Phys. Rev. Lett. **14**, 1072 (1965).

²³K. Würde, A. Mazur, and J. Pollmann, Phys. Rev. B **49**, 7679 (1994).

²⁴G. Jézéquel and I. Pollini, Phys. Rev. B **41**, 1327 (1990).

²⁵S. Bei der Kellen and A. J. Freeman, Phys. Rev. B **54**, 11187 (1996).

²⁶C. Kittel, *Introduction to Solid State Physics*, 6th ed. (Wiley, New York, 1986).

²⁷G. H. O. Daalderop, P. J. Kelly, and M. F. H. Schuurmans, Phys. Rev. B **44**, 12054 (1991).

²⁸A. Sakuma, J. Phys. Soc. Jpn. **63**, 3053 (1994).

²⁹P. Ravindran, A. Kjekshus, H. Fjellvåg, P. James, L. Nordström, B. Johansson, and O. Eriksson, Phys. Rev. B **63**, 144409 (2001).

³⁰A. B. Shick and O. N. Mryasov, Phys. Rev. B **67**, 172407 (2003).

³¹P. E. Blöchl, Phys. Rev. B **50**, 17953 (1994).